

Switching control for a class of nonlinear SISO systems with an application to post-harvest food storage

S. van Mourik, H. Zwart, Twente University,
K.J. Keesman, Wageningen University, The Netherlands

Corresponding author: S. van Mourik
Department of Applied Mathematics
University of Twente, The Netherlands
Phone: +31 (53) 489 3473 , Fax: +31 (53) 489 3800
e-mail: s.vanmourik@ewi.utwente.nl

Abstract For a class of scalar nonlinear systems with switching input a controller is designed using design theory for linear systems. A stability criterion is derived that contains all the physical system parameters, allowing a stability analysis without the need for numerical simulation. The results are motivated by and applied to a model of a bulk storage room for food products. It is shown that for this model a controller with excellent robustness and performance properties can be designed.

1 Introduction

Climate control is an essential part of post-harvest food storage. For maintaining optimal product quality, the most important control parameters are temperature, humidity, CO₂ concentration and ethylene concentration inside the storage room. The most common control inputs are ventilation, cooling, heating, and (de)humidification. The storage room can be ventilated in two ways: ventilation with outside air, or recirculation inside. Forced ventilation is done by fans. Cooling and heating is done by outside air ventilation or by a heat exchanger, and CO₂ and ethylene concentrations are controlled by outside air ventilation. The corresponding mathematical models have complex dynamics due to the airflow and heat- and moisture exchange. Some control inputs are of a discrete nature. Forced air ventilation, for example, is usually realized by a fan that is switched on or off. Generally, standard linear model-based control design is preferred, since it is a mathematically well-understood and practically implementable method, but given the nonlinearities due to the switching input, it is not feasible for this class of systems.

Control strategies that have been developed for storage purposes, are model predictive control (MPC) and fuzzy control. In [5] and [13], MPC algorithms were used for the temperature and humidity control of a bulk storage room with outside air ventilation. Both proposed algorithms are model based and were tested by simulation studies. In [1] a fuzzy controller was tested on a mathematical model. In [3] a sensor based control law for a bulk storage room that was ventilated with outside air was proposed, and in [2] a fuzzy controller was constructed and tested experimentally. In [10] a fuzzy controller was devel-

oped for fruit storage, using neural networks, and in [9] a fuzzy controller was tested experimentally. Further, in [8] a PI controller was designed for CO₂ and O₂ concentrations, and was tested experimentally. In general, the advantages of MPC are that the control algorithm is based on a mathematical model, and that the applicability extends to extremely complicated models. A major drawback is that controller dynamics have to be solved by demanding online numerical computations. Fuzzy controllers are practically easy implementable, but have no mathematical background, and hence controller performance is hard to guarantee.

More general, control design for systems where the switching input is the control parameter, is done by MPC and fuzzy control, as shown above, and switching adaptive control. Stabilizing adaptive controllers are designed in [15, 4] for a large class of nonlinear MIMO systems and for a larger class of MISO systems in [6], with less restrictive assumptions. Here, the control input is switched between two functions that depend continuously on the system states.

In this paper, a controller is designed for a class of piecewise linear systems with switching control inputs. The inputs have fixed values, and are switched at most once in each discrete time interval, in contrast to for example [15, 4, 6]. This paper is organized as follows. In section 2 the model is linearized to a system with the switching moment as input. A controller that dynamically adjusts this input, is designed using standard design theory for linear systems. In section 3 conditions for stability are derived. The stability region is a parametric function of all the system properties, which makes analysis easier. In section 4 the theoretical results are applied to a model of a bulk storage room for harvested products. The control input of this model is the air flow induced by the fan, which is switched on and off on a regular basis. It is shown that the errors that are induced by the linearization cannot destabilize the system. The performance loss due to the linearization is visualized by numerical simulation of the original p.d.e. model, and the approximated piecewise linear system. Both systems are connected to the controller, and simulated under a heavy input disturbance. Since the dynamics of both systems are essentially the same, it is concluded that no essential dynamics are lost, and hence for this model a controller with excellent properties can be designed.

2 System approximation and controller design

Our class of systems is nonlinear, scalar SISO systems of the form

$$\frac{dx}{dt} = A(u)x + B(u). \quad (1)$$

Here, x is the system state, $u = (u_1, u_2)$ the input that attains two discrete values, and A and B scalar functions. The continuous time is divided into discrete time intervals with length τ_f . The control problem is to determine the duration of both inputs. We assume, without loss of generality, that at the start of each time interval $u = u_1$. The input is switched from u_1 to u_2 at time τ ,

with $0 \leq \tau \leq \tau_f$. This gives the following piecewise linear system

$$\frac{dx}{dt}(t) = A(u_1)x(t) + B(u_1) \quad t \in [0, \tau), \quad (2)$$

$$\frac{dx}{dt}(t) = A(u_2)x(t) + B(u_2) \quad t \in [\tau, \tau_f), \quad (3)$$

with $x(\tau^-) = x(\tau^+)$. From now on, the notation $A(u_1) = A_1$ is used, and the subscript denotes the relation with the input. Now τ/τ_f is the fraction of the time that $u = u_1$. The goal is to design a controller that steers x to the desired state x_{opt} by adjusting τ each time interval. Although we want to steer $x(t)$ to x_{opt} , the control action is only based on the state at the beginning of the interval. Thus in the following sections we design a sequence of switching times $\tau \in [n\tau_f, (n+1)\tau_f]$, based on $x(n\tau_f)$ and previous samples, such that $x(n\tau_f) \rightarrow x_{opt}$ for $n \rightarrow \infty$. If the sample time τ_f is small, then this implies that $x(t) - x_{opt}$ will be small for large t . Hence in practice this gives that the state is stabilized around x_{opt} .

Throughout this paper, we assume that A_1 and A_2 are negative, and that $A_1^{-1}B_1 > A_2^{-1}B_2$. Since the choice of A_1, A_2 in (2)–(3) was arbitrary, this imposes no real restrictions.

2.1 System approximation

In this section, the system is approximated, and a controller is designed using standard design theory for linear continuous systems. At the interval $(0, \tau_f)$, the solution to equation (2) at time τ is

$$\begin{aligned} x(\tau) &= x(0) \exp(A_1\tau) + \int_0^\tau \exp(A_1(t-\tau))B_1 dt \\ &= x(0) \exp(A_1\tau) - \left(I - \exp(A_1\tau)\right)A_1^{-1}B_1. \end{aligned} \quad (4)$$

Similarly, the solution to equation (3) becomes

$$x(\tau_f) = x(\tau) \exp(A_2(\tau_f - \tau)) - \left(I - \exp(A_2(\tau_f - \tau))\right)A_2^{-1}B_2. \quad (5)$$

In the interval $[n\tau_f, (n+1)\tau_f]$ we choose the switching time τ^n . We denote the state at time $n\tau_f + \tau^n$ by ξ^n and the state at the time $n\tau_f$ by x^n . So we have

$$\begin{aligned} \xi^n &= \exp(A_1\tau^n)x^n + (\exp(A_1\tau^n) - 1)A_1^{-1}B_1 \\ x^{n+1} &= \exp(A_2(\tau_f - \tau^n))\xi^n + (\exp(A_2(\tau_f - \tau^n)) - 1)A_2^{-1}B_2, \end{aligned} \quad (6)$$

Combining the equations in (6), we find that

$$x^{n+1} = f(x^n, \tau^n). \quad (7)$$

The switching time is chosen such that the system is in the desired state x_{opt} for all time instances $n\tau_f$. The following lemma shows that for any $x_{opt} \in [-A_1^{-1}B_1, -A_2^{-1}B_2]$ there exists a unique switching time $\tau_{opt} \in (0, \tau_f)$ such that

$$x_{opt} = f(x_{opt}, \tau_{opt}). \quad (8)$$

Lemma 2.1. Consider the system (6). Then equation (8) has a solution $\tau_{opt} \in [0, \tau_f]$ if and only if

$$-A_1^{-1}B_1 \leq x_{opt} \leq -A_2^{-1}B_2. \quad (9)$$

Furthermore, when (9) holds, then the solution τ_{opt} is unique.

Proof. See the appendix. \square

Since we will not start at x_{opt} and since disturbances may drive x away from the desired state x_{opt} , we want to design a feedback control law for τ^n , such that $x^n \rightarrow x_{opt}$. For this we linearize system (7) around x_{opt}, τ_{opt} , i.e. we set

$$\begin{aligned} \tau^n &= \tau_{opt} + \tau_{var}^n \\ x^n &= x_{opt} + x_{var}^n. \end{aligned} \quad (10)$$

The linearized system equals

$$\begin{aligned} x_{var}^{n+1} &= \frac{\partial f}{\partial x^n}(x_{opt}, \tau_{opt})x_{var}^n + \frac{\partial f}{\partial \tau^n}(x_{opt}, \tau_{opt})\tau_{var}^n \\ &= A_d x_{var}^n + B_d \tau_{var}^n. \end{aligned} \quad (11)$$

We have that

$$\begin{aligned} A_d &= \exp(A_2(\tau_f - \tau_{opt}) + A_1\tau_{opt}) \\ B_d &= -A_2 \exp(A_2(\tau_f - \tau_{opt}))\xi(\tau_{opt}) \\ &\quad + \exp(A_2(\tau_f - \tau_{opt})) \left(A_1 \exp(A_1\tau_{opt})x_{opt} + B_1 \exp(A_1\tau_{opt}) \right) \\ &\quad - B_2 \exp(A_2(\tau_f - \tau_{opt})) \\ &= -A_2 x_{opt} - B_2 + \\ &\quad \exp(A_2(\tau_f - \tau_{opt})) \left(A_1 \exp(A_1\tau_{opt})x_{opt} + B_1 \exp(A_1\tau_{opt}) \right). \end{aligned} \quad (12)$$

Since A_1 and A_2 are negative, and since $0 \leq \tau_{opt} \leq \tau_f$, we see that $A_d \in (0, 1)$. We note that any nonlinear MIMO system with switching input can be brought to the form of (11), and hence enable linear (discrete) control design. However, we consider scalar systems of the form (1) since they allow a rigorous stability analysis that results in a stability area that consists of analytical expressions that contain physical knowledge of the system.

2.2 Controller design

In the appendix we show how by using a standard PI controller on an approximate continuous time system, a controller can be designed for our discrete time system. Our PI-based controller in discrete time is

$$\begin{aligned} \zeta^{n+1} &= -\frac{(A_d - 1)^2}{B_d} x_{var}^n + \zeta^n \\ \tau_{var}^n &= \frac{A_d - 1}{B_d} x_{var}^n + \zeta^n. \end{aligned} \quad (13)$$

From the second equation in (13) it is clear that (x_{var}^n, ζ^n) converges to zero if and only if $(x_{var}^n, \tau_{var}^n)$ converges to zero. Using (13) and (11) we have

$$\begin{aligned}
\tau_{var}^{n+1} &= \frac{A_d - 1}{B_d} (A_d x_{var}^n + B_d \tau_{var}^n) - \frac{(A_d - 1)^2}{B_d} x_{var}^n + \zeta^n \\
&= \frac{A_d - 1}{B_d} \left(A_d x_{var}^n - (A_d - 1) x_{var}^n + B_d \tau_{var}^n \right) + \tau_{var}^n - \frac{A_d - 1}{B_d} x_{var}^n \\
&= (A_d - 1) \tau_{var}^n + \tau_{var}^n \\
&= A_d \tau_{var}^n.
\end{aligned} \tag{14}$$

Thus the closed loop system for x_{var}^n and τ_{var}^n is

$$\begin{aligned}
x_{var}^{n+1} &= A_d x_{var}^n + B_d \tau_{var}^n \\
\tau_{var}^{n+1} &= A_d \tau_{var}^n.
\end{aligned} \tag{15}$$

Since $A_d \in (0, 1)$ this is stable. In the following section we investigate the stability of the controller (13) on the original system.

3 Stability analysis

In this section we prove that the controller (13) stabilizes the original system (7). The control action on the original system is modified such that realistic time switches are applied to the original system. The rules are

$$\begin{aligned}
&\text{If } \tau_{var}^n + \tau_{opt} > \tau_f, \text{ then } \tau^n = \tau_f \\
&\text{If } \tau_{var}^n + \tau_{opt} < 0, \text{ then } \tau^n = 0 \\
&\text{If } 0 \leq \tau_{var}^n + \tau_{opt} \leq \tau_f, \text{ then } \tau^n = \tau_{var}^n + \tau_{opt}.
\end{aligned} \tag{16}$$

Next we show that if τ^n is chosen according to these rules, then x^n stays bounded. Later we show that $x^n \rightarrow x_{opt}$.

Lemma 3.1. *Let τ^n be a sequence in the interval $[0, \tau_f]$ and let x^0 be given. For any $\delta > 0$ there exists a N such that $x^N \in (-A_1^{-1}B_1 - \delta, -A_2^{-1}B_2 + \delta)$ for $n \geq N$. Here x^n is the solution of (7).*

Proof. See the appendix. □

Using the linearized model (11) we can write (7) as

$$x_{var}^{n+1} = A_d x_{var}^n + (B_d + \varepsilon(x_{var}^n, \tau_{var}^n)) \tau_{var}^n. \tag{17}$$

Here we have used that (7) is linear in x . Similar as in (14), we obtain the following difference equation for τ_{var}

$$\tau_{var}^{n+1} = \left(A_d + \frac{A_d - 1}{B_d} \varepsilon(x_{var}^n, \tau_{var}^n) \right) \tau_{var}^n. \tag{18}$$

Here ε is the error induced by linearization. Our closed loop system becomes

$$\begin{aligned} x_{var}^{n+1} &= A_d x_{var}^n + (B_d + \varepsilon(x_{var}^n, \tau_{var}^n)) \tau_{var}^n \\ \tau_{var}^{n+1} &= \left(A_d + \frac{A_d - 1}{B_d} \varepsilon(x_{var}^n, \tau_{var}^n) \right) \tau_{var}^n. \end{aligned} \quad (19)$$

We know from Lemma 3.1 that $(x_{var}^n, \tau_{var}^n)$ will lie in a bounded set. Using the second equation of (19), we conclude that if ε is sufficiently small, then $\tau_{var}^n \rightarrow 0$. Since ε contains higher order terms, and since $\varepsilon(0, 0) = 0$, the condition that ε is small in a neighbourhood of $(0, 0)$ is not a strong assumption. Concluding, we have

Theorem 3.2. *Consider equation (19). Let $\Omega = \{(x_{var}, \tau_{var}) \mid x_{var} + x_{opt} \in [-A_1^{-1}B_1, -A_2^{-1}B_2]\}$ and $\tau_{var} + \tau_{opt} \in [0, \tau_f]\}$. If*

$$\sup_{(x_{var}, \tau_{var}) \in \Omega} \left| A_d + \frac{A_d - 1}{B_d} \varepsilon(x_{var}, \tau_{var}) \right| < 1, \quad (20)$$

then (19) is asymptotically stable.

4 Application to food storage

In this section, the controller design and the stability analysis from the previous section are applied to a model of a bulk storage room for harvested food products.

4.1 The model

In this subsection the (approximated) model that was derived and validated in [12], is described. The storage room model is divided into two parts, namely the shaft and the bulk, see Figure 1. The resulting model equations are

$$V \frac{\partial T_0(t)}{\partial t} = -\Phi \alpha(\Phi) (T_a(L, t) - T_c(t)) + \Phi T_a(L, t) - \Phi T_0(t) \quad (21)$$

$$\frac{\partial T_a(x, t)}{\partial t} = -v \frac{\partial T_a(x, t)}{\partial x} + M_4 (T_p(x, t) - T_a(x, t)) \quad (22)$$

$$\frac{\partial T_p(R, x, t)}{\partial t} = A_p T_p(R, x, t) + B_p T_a(x, t) \quad (23)$$

$$T_a(0, t) = T_0(t). \quad (24)$$

This will be further referred to as the *nominal system*. The control input is the air flux $\Phi(t)$ that is generated by the fan, and this switches between Φ_1 and Φ_2 . Equation (21) describes the temperature dynamics inside the shaft. V is the volume of the shaft, $T_a(L, t)$ the air temperature at the top of the bulk, $T_c(t)$ the temperature of the cooling element inside the heat exchanger, ρ_a the air density, c_a the heat capacity of air. The dimensionless function α

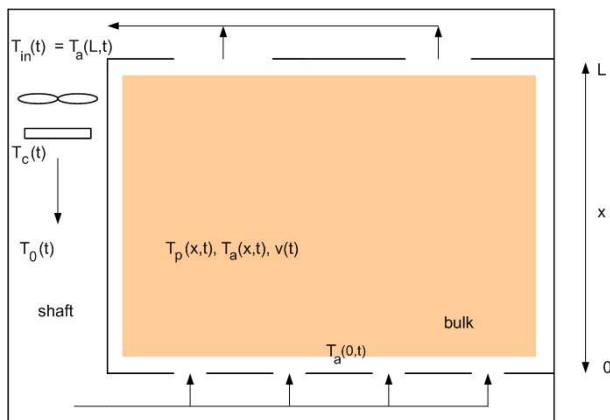


Figure 1: Schematic representation of a bulk storage room.

denotes the effectiveness of the cooling device: $\alpha = 1$ implies that the incoming air $T_{in}(t)$ is totally cooled down (or heated up) to $T_c(t)$, while $\alpha = 0$ implies that the incoming air is not cooled at all. Here, α is assumed to be constant. Equation (22) describes the temperature dynamics of the air inside the bulk. The two r.h.s. terms in equation (22) denote the convection of heat and the heat exchange between product surface and air, respectively. Here, x denotes the height in the bulk, that varies from 0 to L . Further, $M_4 = \frac{h(v)A_{ps}}{\gamma\rho_a c_a}$, with γ the bulk porosity, and A_{ps} the product surface area per bulk volume. The heat transfer coefficient $h(v)$ depends on v via the implicit relation (see [14])

$$\text{Nu} = (0.5\text{Re}^{1/2} + 0.2\text{Re}^{2/3})\text{Pr}^{1/3} \quad (25)$$

for $10 < \text{Re} < 10^4$, with Nu, Re and Pr the Nusselt, Reynolds and Prandtl number, see section 6. The average velocity inside the bulk is $v = \frac{\Phi}{A_f\gamma}$, with A_f the area of the bulk floor. Equation (23) describes the temperature dynamics of the product skin (which represents the product temperature) at height x inside the bulk. The expressions for A_p and B_p are listed in the appendix. Parameters a and Bi are respectively the heat production of the products and the Biot number. The model predictions were found to be accurate when compared to experimental results. System (21)–(24) was approximated by using timescale decomposition and transfer function approximation to

$$\frac{dT_p(L,t)}{dt} = A(\Phi(t))T_p(L,t) + B(\Phi(t)), \quad (26)$$

with $T_p(L,t)$ the product temperature at the top of the bulk. The expressions for A and B are given in the appendix. The values of the physical parameters are listed in Table 1. In Table 2 the corresponding numerical values of the key parameters are listed.

α	0.4	A_f	5 m
R	$3.25 \cdot 10^{-2}$ m	V	10 m ³
Φ_1	1 m ³ /s	Φ_2	0.001 m ³ /s
λ_p	0.55 J/s m K	ρ_p	1014 kg/m ³
a	$3.1 \cdot 10^{-5}$ J/s kg K	A_{ps}	49 m ²
γ	0.39	c_p	$3.6 \cdot 10^3$ J/kg K
T_c	275 K	c_a	$2 \cdot 10^3$ J/kg K
L	4 m		

Table 1: Physical parameters of a bulk storage room with potatoes. Specific data were taken from [5, 14, 11].

A_1	$-2 \cdot 10^{-5}$ 1/s	A_2	$-2 \cdot 10^{-8}$ 1/s
B_1	$6.6 \cdot 10^{-3}$ K/s	B_2	$8.1 \cdot 10^{-6}$ K/s
A_d	$1.0 - 3 \cdot 10^{-4}$	B_d	$-1.2 \cdot 10^{-4}$ K/s
τ_f	600 s	τ_{opt}	12.2 s
$T_{p,opt}$	280 K		

Table 2: Numerical key parameter values.

4.2 Controller

The controller measures the product temperature at the top of the bulk, $T_p(L, t)$. The optimal switching time corresponds to $T_p(L, t) = T_{p,opt}$. Realistic disturbances in the air temperature $T_0(t)$ is caused by open doors, heat leakage through the walls, etcetera. For mathematical simplicity we assume that the disturbances in air temperature occur in the vicinity of the heat exchanger, and that they therefore act on the system as the temperature of the cooling element T_c . For design purposes, we look at the crossover frequency of the transfer function from T_c to $T_p(L)$. In [12] it was shown that this transfer function has a crossover frequency of $k = -A^*(\Phi)$. For simplicity, we take the average of k w.r.t. the switching time, which gives

$$k_{av} = \frac{\tau_{opt}}{\tau_f} k(\Phi_1) + \frac{\tau_f - \tau_{opt}}{\tau_f} k(\Phi_2). \quad (27)$$

It turns out that this is practically the same crossover frequency as in G . This means that, from a classic control design point of view, the perturbations act on the system as depicted in Figure 3. Therefore, the controller design as proposed in section 2.2 is appropriate for the bulk storage room model.

4.3 Stability

In this section the influence of the linearization error on the stability is investigated. We define the linearization as in (11), with the variable x replaced with $T_p(L)$. Also, $T_p(L)$ is denoted by T_p for convenience. We recall the system (19)

with x_{var} replaced with $T_{p,var}$

$$\begin{aligned} T_{p,var}^{n+1} &= A_d T_{p,var}^n + (A_d + \varepsilon) \tau_{var}^n \\ \tau_{var}^{n+1} &= (A_d + \varepsilon) \tau_{var}^n. \end{aligned} \quad (28)$$

We have that

$$\begin{aligned} \varepsilon &= \frac{1}{2} \frac{\partial^2 f}{\partial T_p^n \partial \tau^n}(T_{p,opt}, \tau_{opt}) T_{p,var}^n + \frac{1}{2} \frac{\partial^2 f}{\partial \tau^n \partial T_p^n}(T_{p,opt}, \tau_{opt}) T_{p,var}^n \\ &\quad + \frac{1}{2} \frac{\partial^2 f}{\partial (\tau^n)^2}(T_{p,opt}, \tau_{opt}) \tau_{var}^n + \text{h.o.t.} \end{aligned} \quad (29)$$

We neglect the higher order terms of ε , which gives

$$\begin{aligned} \varepsilon &= \frac{1}{2} \left((A_1 - A_2) \alpha_2 - A_2 + A_1 \alpha_2 \right) T_{p,var}^n + \\ &\quad \left(\frac{1}{2} (A_1 - A_2) \left((A_1 - A_2) \alpha_2 T_{p,opt} - \frac{A_2 B_1}{A_1} \alpha_2 + B_1 \alpha_2 \right) \right. \\ &\quad \left. - \frac{1}{2} A_2 \left(\frac{A_2 B_1}{A_1} - B_2 \right) \exp(A_2(\tau_f - \tau_{opt})) \right) \tau_{var}^n, \end{aligned} \quad (30)$$

with $\alpha_2 = \exp(A_2(\tau_f - \tau_{opt}) + A_1 \tau_{opt})$. Numerical evaluation gives

$$\varepsilon = -2.4 \cdot 10^{-5} T_{p,var} + 7.9 \cdot 10^{-8} \tau_{var}. \quad (31)$$

We have that $A_d = 1 - 3 \cdot 10^{-4}$, and $B_d = 6.5 \cdot 10^{-3}$, so the stability criterion of Theorem 3.2 $|A_d + \frac{A_d - 1}{B_d} \varepsilon| < 1$ becomes $|1 - 3 \cdot 10^{-4} + 4.6 \cdot 10^{-2} \varepsilon| < 1$, which is fulfilled if $|\varepsilon| < 64.6$. We have that $0 < \tau_{var} < 600$, according to (16), and that T_p will converge to the range $(-A_1^{-1} B_1 - \delta, -A_2^{-1} B_2 + \delta)$ for any δ , by Lemma 3.1. Since for our case $(-A_1^{-1} B_1, -A_2^{-1} B_2) = (275.1, 398.2)$, we have that $|T_{p,var}| < 123.1$ for any choice of $T_{p,opt}$. Altogether, $T_{p,var}$ and τ_{var} cannot grow large enough to destabilize the system, and hence the system is asymptotically stable according to Theorem 3.2.

4.4 Simulation study

In the previous section the stability robustness was analyzed, and in this section we analyze the loss of performance due to the linearization. This is done by connecting controller (36) to the linearized system (32) and to the nominal system (21)–(24). The differences in $T_p(L, t)$ and $\tau(t)$ should give an indication whether any essential dynamics is discarded. The two controlled systems are simulated numerically. For the spatial discretisations, a forward Euler step was used, and the dynamics in time were computed inside the Matlab Simulink environment using an ode45 Dormand-Prince algorithm. Further, a heavy input disturbance d was added, such that the system dynamics were clearly visible. The initial product temperature was set uniform at 285 K, while the optimal product temperature is 280 K. The input disturbance is $d = a \sin(\omega t)$, with

$a = 10 \text{ s}$, and $\omega = 3 \cdot 10^{-6} \text{ Hz}$.

The dynamics of $\tau(t)$ and $T_p(L, t)$ are shown in Figure 2. For both controlled systems the dynamics of $T_p(L, t)$ and $\tau(t)$ are more or less the same, indicating that the approximation errors in the approximation steps from (21)–(24) to (32) do not discard any essential dynamics. Even when initially the product temperature differs considerably from the linearization point of 280 K , the differences are small. Furthermore, the controller seems to perform quite well under these large input disturbances. For various frequencies of d similar results were obtained. The differences in system dynamics increase with the amplitude, since then the linearization error becomes larger.

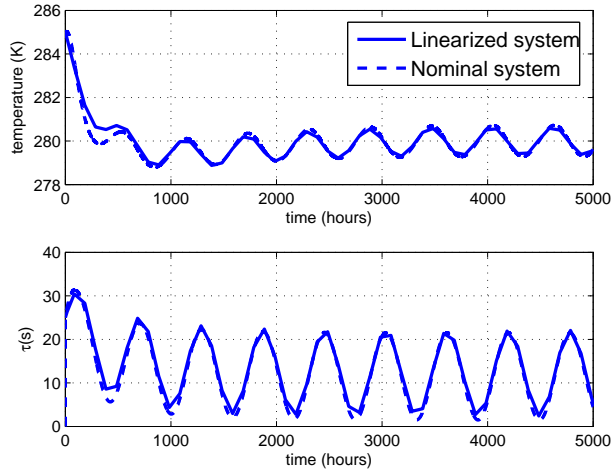


Figure 2: $T_p(L, t)$ (upper left) and $\tau(t)$ (upper right) of the linearized controlled system, and $T_p(L, t)$ (bottom left) and $\tau(t)$ (bottom right) of the nominal controlled system.

5 Conclusions

We showed that for a large class of nonlinear scalar systems with discrete input, it is possible to make an approximation that allows the design of a linear controller that controls the switching time of the input. This is done by a linearization, and the linearization points are the optimal switching time that corresponds to the optimal state, and the optimal state. Lemmas 2.1 and 3.1 give conditions for the existence of such a linearization point, state its uniqueness, and guarantee that the state is bounded. Theorem 3.2 gives the condition for asymptotic stability of the controlled system. The conditions are in analytical form, which gives a more structural insight into the influence of errors and

perturbations on the stability.

As an example, a controller was designed and connected to a temperature model of a bulk storage room. For controller design, the original (or nominal) model was linearized. It was shown that the stability cannot be jeopardized by the linearization error. Numerical simulations show that under large input disturbances the nominal and the approximated system have similar dynamics in T_p and τ . This also holds for different physical parameters and disturbance frequencies, indicating that the linearization does not discard any essential dynamics. Hence a controller with excellent properties can be designed for the bulk storage room model.

The linearization and the controller design can be applied to any system. However, for more complex systems, such as higher order systems, the controller design and the stability analysis do generally not result in parametric expressions, and will therefore be more numerically involved. Nevertheless, a next step would be the design of a switching input controller for higher order systems, together with a numerical stability analysis.

5.1 Acknowledgement

This work was supported by the Technology Foundation STW under project number WWI.6345.

References

- [1] K. Gottschalk. Mathematical modelling of the thermal behaviour of stored potatoes and developing of fuzzy control algorithms to optimise the climate in storehouses. *Acta horticulturae: technical communications of ISHS*, 10:331–340, 1996.
- [2] K. Gottschalk, L. Nagy, and I. Farkas. Improved climate control for potato stores by fuzzy controllers. *Computers and electronics in agriculture*, 40:127–140, 2003.
- [3] K. Gottschalk and W. Schwarz. Klimaautomatisierung für kartoffellager. *Landtechnik*, 3:132–133, 1997.
- [4] H. Hespana and A.S. Morse. Supervision of families of nonlinear controllers. In *35th IEEE conference on decision control*, volume 4, pages 3771–3773, 1996.
- [5] K.J. Keesman, D. Peters, and L.J.S. Lukasse. Optimal climate control of a storage facility using local weather forecasts. *Control Engineering Practice*, 11:505–516, 2003.
- [6] E.B. Kosmatopoulos and P.A. Ioannou. Robust switching adaptive control of multi-input nonlinear systems. *IEEE transactions on automatic control*, 47(4):610–624, 2002.

- [7] H. Kwakernaak. *Trends in control - a European perspective*, chapter Symmetries in control design, pages 17–51. Springer, Heidelberg, 1995.
- [8] N.R. Markarian, C. Vigneault, Y. Gariépy, and T.J. Rennie. Computerized monitoring and control for a research controlled-atmosphere storage facility. *Computers and electronics in agriculture*, 39:23–37, 2003.
- [9] T. Morimoto and Y. Hashimoto. An intelligent control for greenhouse automation, oriented by the concepts of spa and sfa - an application to a post-harvest process. *Computers and electronics in agriculture*, 29:3–20, 2000.
- [10] T. Morimoto, J. Suzuki, and Y. Hashimoto. Optimization of a fuzzy controller for fruit storage using neural networks and genetic algorithms. *Engineering applications in artificial intelligence*, 10:453–461, 1997.
- [11] A. Rastovski and A. van Es et al. *Storage of potatoes, Post-harvest behaviour, store design, storage practice, handling*. Pudoc Wageningen, 1987.
- [12] H.J. Zwart S. van Mourik and K.J. Keesman. Analytical control law for a food storage room. Technical Report ISSN 1874-4850, Twente university, 2007.
- [13] G.J.C. Verdijck. *Product quality control*. PhD thesis, University of Eindhoven, 2003.
- [14] Y. Xu and D. Burfoot. Simulating the bulk storage of foodstuffs. *Journal of food engineering*, 39:23–29, 1999.
- [15] B. Yao and M. Tomizuka. Adaptive robust control of a class of multivariable nonlinear systems. In *IFAC world congress*, volume F, pages 1360–1375, 1996.

6 Appendix

6.1 Controller design

The following strategy is used. Equation (11) is approximated by a continuous system, by taking $\tau_f \rightarrow 0$. The idea is that the dynamics of x are slow on $(0, \tau_f)$, and therefore $\frac{\partial x}{\partial t} \approx \frac{x^{n+1} - x^n}{\tau_f}$. We start by rewriting (11) as

$$\frac{x_{var}^{n+1} - x_{var}^n}{\tau_f} = A_{lin} x_{var}^n + B_{lin} \tau_{var}^n, \quad (32)$$

with $A_{lin} = \frac{A_d - 1}{\tau_f}$, and $B_{lin} = \frac{B_d}{\tau_f}$. We approximate it by a continuous system, by taking $\tau_f \rightarrow 0$, so (32) becomes

$$\frac{dx_{var}(t)}{dt} = A_{lin} x_{var}(t) + B_{lin} \tau_{var}(t). \quad (33)$$

For (33) it is now possible to design a controller by standard linear theory. For the formulation of design specifications, system (33) is transformed into the Laplace frequency domain to

$$\begin{aligned}\widehat{x}_{var}(s) &= \frac{B_{lin}}{-A_{lin} + s} \widehat{\tau}_{var}(s) \\ &= G(s) \widehat{\tau}_{var}(s).\end{aligned}\quad (34)$$

In this section it is assumed for simplicity, that there is only one disturbance, d , which acts on the input τ_{var} . Figure 3 shows the interconnection of $G(s)$ and the controller $K(s)$, together with the input disturbance. Various designs are possible, e.g. LQG or optimal control design. We propose the following design specifications that are standard for linear SISO systems (see for example [7] for more details).

- The sensitivity function $S = \frac{1}{1+K(s)G(s)}$ from d to x_{var} should be small for low frequencies, and close to 1 for high frequencies for good performance.
- A very high crossover frequency of S will result in a very fast controller, with the tradeoff that the performance and stability will be poor.

Input disturbances with a higher frequency than the crossover frequency of G are already attenuated by G . Therefore, a good choice would be that S is small up to the crossover frequency of G : $-A_{lin}$. In other words, we have to find K such that

$$\frac{1}{1 + G(s)K(s)} = \frac{\tilde{s}}{1 + \tilde{s}}, \quad (35)$$

with $\tilde{s} = \frac{s}{-A_{lin}}$. In this way, S_2 is small for all frequencies, S is small for frequencies up to $s = -A_{lin}$, and S tends to 1 for high frequencies. Straightforward calculation gives the PI controller

$$\begin{aligned}K(s) &= \frac{A_{lin} - s}{\frac{B_{lin}}{A_{lin}} s} \\ \Leftrightarrow \widehat{\tau}(s) &= \left(-\frac{A_{lin}^2}{B_{lin}s} + \frac{A_{lin}}{B_{lin}}\right) \widehat{x}_{var}(s).\end{aligned}\quad (36)$$

With the substitution

$$\widehat{\zeta}(s) = -\frac{A_{lin}^2}{B_{lin}s} \widehat{x}_{var}(s) \quad (37)$$

our controller in discrete time becomes

$$\begin{aligned}\frac{\zeta^{n+1} - \zeta^n}{\tau_f} &= -\frac{A_{lin}^2}{B_{lin}} x_{var}^n \\ \tau_{var}^n &= \zeta^n + \frac{A_{lin}}{B_{lin}} x_{var}^n.\end{aligned}\quad (38)$$

Note that the controller is an *explicit* parametric function of all the system characteristics. Figure 3 shows the controlled system with input disturbance d schematically.

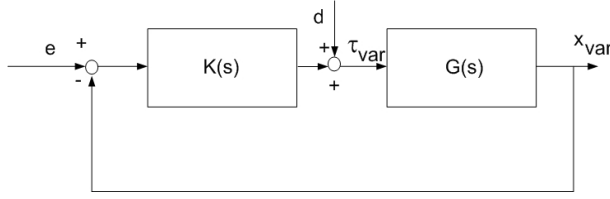


Figure 3: Schematic overview of the controlled system with input disturbance d .

6.2 Proofs

6.2.1 Proof of lemma 2.1

Using (6) we can write $f(x, \tau)$ as

$$f(x, \tau) = f_1(\tau)x + f_2(\tau). \quad (39)$$

Further, it is not hard to see that for $\tau \in [0, \tau_f]$ $f_1(\tau) \in (0, 1)$, and

$$\begin{aligned} f_2(0) &= (\exp(A_2\tau_f) - 1)A_2^{-1}B_2 \\ f_1(\tau_f) &= (\exp(A_1\tau_f) - 1)A_1^{-1}B_1. \end{aligned} \quad (40)$$

Solving

$$x_{opt} = f_1(\tau)x_{opt} + f_2(\tau) \quad (41)$$

for $\tau \in [0, \tau_f]$ is possible if and only if

$$x_{opt} = \frac{f_2(\tau)}{1 - f_1(\tau)} \quad (42)$$

is solvable for $\tau \in [0, \tau_f]$. Since the right hand side is a continuous function of τ , we see that solving (42) is possible if and only if x_{opt} lies in the range of $f_2/(1 - f_1)$. We have that

$$\begin{aligned} \frac{f_2(0)}{(1 - f_1(0))} &= -A_2^{-1}B_2 \\ \frac{f_2(\tau_f)}{(1 - f_1(\tau_f))} &= -A_1^{-1}B_1. \end{aligned} \quad (43)$$

Thus if x_{opt} lies between these values, then (42) is solvable. If the range of $f_2/(1 - f_1)$ for $\tau \in [0, \tau_f]$ would be larger, then

$$\begin{aligned} \frac{f_2(\tau)}{(1 - f_1(\tau))} &= -A_2^{-1}B_2 \quad \text{or} \\ \frac{f_2(\tau)}{(1 - f_1(\tau))} &= -A_1^{-1}B_1 \end{aligned} \quad (44)$$

must be solvable for at least two $\tau \in [0, \tau_f]$. We show that this is not possible. We do this for the second equation, the first one goes similarly. Using (44) in (6) gives

$$\begin{aligned}\xi &= -A_1^{-1}B_1 \\ -A_1^{-1}B_1 &= \exp(A_2(\tau_f - \tau))\xi^n + (\exp(A_2(\tau_f - \tau)) - 1)A_2^{-1}B_2 \\ \Leftrightarrow A_1^{-1}B_1 &= \exp(A_2(\tau_f - \tau))A_1^{-1}B_1 - (\exp(A_2(\tau_f - \tau)) - 1)A_2^{-1}B_2 \\ \Leftrightarrow A_1^{-1}B_1 &= (\exp(A_2(\tau_f - \tau)) - 1)(A_1^{-1}B_1 - A_2^{-1}B_2).\end{aligned}\quad (45)$$

Since $A_1^{-1}B_1 \neq A_2^{-1}B_2$, we must have $\exp(A_2(\tau_f - \tau)) - 1 = 0$, which gives $\tau = \tau_f$. Now we will prove the uniqueness of τ_{opt} . Assume that τ_1 and τ_2 are times such that

$$x_{opt} = f(x_{opt}, \tau_i) \quad i = 1, 2. \quad (46)$$

Assume that $\tau_1 < \tau_2 \leq \tau_f$, and let

$$\xi_i = \exp(A_1\tau_i)x_{opt} + A_1^{-1}B_1(\exp(A_1\tau_i) - 1) \quad i = 1, 2. \quad (47)$$

We observe from (6) that

$$\xi_i + A_1^{-1}B_1 = \exp(A_1\tau_i)(x_{opt} + A_1^{-1}B_1) \quad (48)$$

$$x_{opt} + A_2^{-1}B_2 = \exp(A_2(\tau_f - \tau_i))(\xi_i + A_2^{-1}B_2) \quad (49)$$

Since $A_1 < 0$, and since $\tau_1 < \tau_2$, we have by (48) and $x_{opt} > -A_1^{-1}B_1$ that

$$\xi_1 + A_1^{-1}B_1 > \xi_2 + A_1^{-1}B_1 \quad (50)$$

This implies that

$$\xi_2 + A_2^{-1}B_2 > \xi_1 + A_2^{-1}B_2. \quad (51)$$

Now using (49) and the fact that $\tau_f - \tau_1 > \tau_f - \tau_2$ we find

$$\exp(A_2(\tau_f - \tau_2))(\xi_2 + A_2^{-1}B_2) > \exp(A_2(\tau_f - \tau_1))(\xi_1 + A_2^{-1}B_2). \quad (52)$$

However, both expressions must be equal to x_{opt} . Hence τ_1 cannot be unequal to τ_2 . \square

6.2.2 Proof of lemma 3.1

We want to show that for some N $x^N \in [-A_1^{-1}B_1 - \delta, -A_2^{-1}B_2 + \delta]$ for any $\delta > 0$. Suppose that this does not hold, then $x^n \notin [-A_1^{-1}B_1 - \delta, -A_2^{-1}B_2 + \delta]$ for all n . Suppose

$$x^0 < -A_1^{-1}B_1 - \delta \Rightarrow (48) \quad \xi^0 < -A_1^{-1}B_1 - \delta \quad (53)$$

which implies that $x_1 < -A_2^{-1}B_2$. Since $x^1 \notin [-A_1^{-1}B_1 - \delta, -A_2^{-1}B_2 + \delta]$ we have

$$x^1 < -A_1^{-1}B_1 - \delta. \quad (54)$$

Furthermore, $x^0 < x^1$. Repeating the above argument gives

$$x^0 < x^1 < x^2 \dots x^n \leq -A_1^{-1}B_1 - \delta. \quad (55)$$

Hence $x^n \rightarrow x^\infty \leq -A_1^{-1}B_1 - \delta$. Similarly, $\xi^n \rightarrow \xi^\infty \leq -A_1^{-1}B_1 - \delta$. From (48) we conclude that if x and ξ both converge, then so does τ . So $\tau^n \rightarrow \tau^\infty$. Thus we have that (x^∞, τ^∞) is a fixed point that satisfies $x^\infty = f(x^\infty, \tau^\infty)$ and $x^\infty < -A_1^{-1}B_1$. Lemma 2.1 implies that $x^\infty \geq -A_1^{-1}B_1$. \square

6.3 Parameters

Φ	air flow through shaft (m^3/s)
α	cooling effectiveness (K)
α_{th}	thermal diffusivity of air ($1.87 \cdot 10^{-5} m^2/s$)
γ	porosity (m^3/m^3)
λ_a	conduction of air ($2.43 \cdot 10^{-2} W/m K$)
λ_p	conduction of product ($W/m K$)
ν	kinematic viscosity of air ($1.35 \cdot 10^{-5} m^2/s$)
ρ_a	air density ($1.27 kg/m^3$)
ρ_p	produce density (kg/m^3)
τ	switching time (s)
τ_f	length of switching interval (s)
A_f	floor area of the bulk (m^2)
A_{ps}	produce surface per bulk volume (m^2/m^3)
Bi	Biot number $\frac{2hR}{\lambda_a}$
L	bulk height (m)
L_2	$R * \gamma(1 - \gamma)$, char. length (m)
Nu	Nusselt number $\frac{2hR}{\lambda_a}$
Pr	Prandtl number $\frac{\nu}{\alpha_{th}}$
R	product radius (m)
Re	Reynolds number $\frac{vL_2}{\nu}$, [14]
T_a	air temperature in the bulk (K)
T_c	cooling element temperature (K)
T_{ini}	initial temperature (K)
T_p	produce temperature (K)
V	volume of shaft (m^3)
a	product heat production ($J/kg s K$)
b	product heat production ($J/kg s$)
c_a	heat capacity of air ($1 \cdot 10^3 J/kg K$)
c_p	heat capacity of produce ($J/kg K$)
h	heat transfer coefficient ($W/m^2 K$)
v	air velocity inside the bulk (m/s)

6.4 Expressions

$$\begin{aligned}
 A & A^* \\
 B & B^* T_c \\
 A^* & \frac{\tilde{A}_p A_p}{A_p + \tilde{A}_p} \\
 B^* & - \frac{\tilde{B}_p B_p}{A_p + \tilde{A}_p} T_c \\
 \tilde{A}_p & - \frac{A_p^2}{M_5 B_p} + \frac{A_p^2 (1-\alpha)}{M_5 B_p} \exp\left(M_5 \left(\frac{B_p + A_p}{-A_p}\right)\right) \\
 \tilde{B}_p & \frac{\alpha A_p^2}{M_5 B_p} \exp\left(M_5 \left(\frac{B_p + A_p}{-A_p}\right)\right) \\
 A_p & - \frac{2M_3 \cot(M_3) - 2 + \text{Bi}}{\frac{R^2}{M_1} \cot^2(M_3) + \frac{R^2}{M_1} - \frac{M_3}{M_2} \cot(M_3)} \\
 B_p & \frac{\text{Bi}}{\frac{R^2}{M_1} \cot^2(M_3) + \frac{R^2}{M_1} - \frac{M_3}{M_2} \cot(M_3)} \\
 M_1 & \frac{\lambda_p}{\rho_p c_p} \\
 M_2 & \frac{a}{c_p} \\
 M_3 & \sqrt{M_2 / M_1} R \\
 M_4 & \frac{h A_p}{\gamma \rho_a c_a} \\
 M_5 & \frac{M_4 L}{v} \\
 v & \frac{\Phi}{A_f}
 \end{aligned}$$